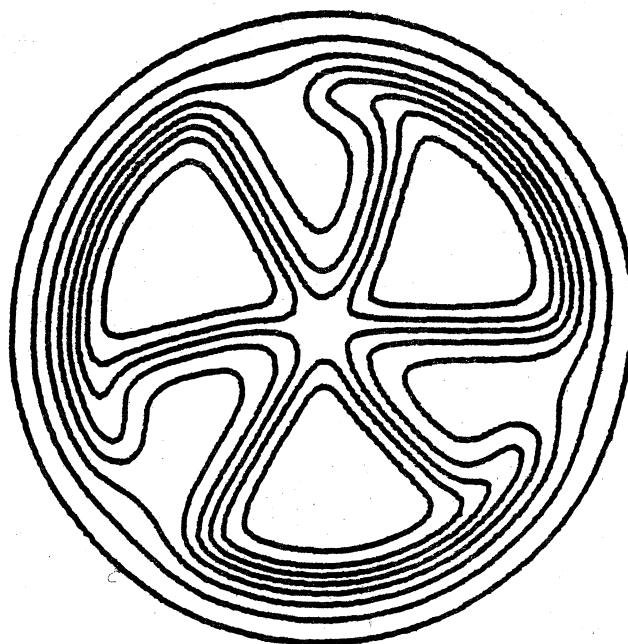


MICHIGAN STATE UNIVERSITY

CYCLOTRON LABORATORY

A STUDY OF THE NUCLEAR STRUCTURE OF  $^{36}\text{Cl}$   
WITH THE (p,d) REACTION

J.A. RICE, B.H. WILDENTHAL, and B.M. FREEDOM



## I. INTRODUCTION

The present work is part of a comprehensive study of doubly-odd nuclei in the sd-shell via the (p,d) reaction. 1-4 This study is motivated by the fact that current nuclear structure theories experience considerably more difficulty in accounting for the properties of the doubly-odd nuclei in this region than for those of the doubly-even or even-odd nuclei. The features of the low-lying energy levels of a nucleus which are revealed by single-nucleon transfer experiments are central to understanding the nuclear structure of the system. Our aim is to obtain complete and accurate sets of neutron-pickup spectroscopic factors so that unambiguous and definitive tests can be made of this aspect of current nuclear models. The present data for  $^{36}\text{Cl}$  also provide a new and more accurate set of excitation energies for  $^{36}\text{Cl}$  than previously existed and yield several new or revised assignments for  $k_n$  and  $\pi$ .

## II. EXPERIMENTAL PROCEDURE

Targets for the present experiment were prepared by vacuum evaporation of NaCl, enriched to >96.5% in  $^{37}\text{Cl}$ , on to 30  $\mu\text{gm}/\text{cm}^2$  carbon foil backings. The targets were bombarded with 35 Mev protons from the MSU sector-focused cyclotron and the reaction products analyzed with a split-pole magnetic spectrograph. Deuteron spectra were measured both with a position-sensitive single-wire proportional counter and with 25-micron-thick nuclear emulsion plates.

A Study of the Nuclear Structure of  $^{36}\text{Cl}$  with the (p,d) Reaction\*

J.A. Rice and B.H. Wildenthal  
Cyclotron Laboratory, Department of Physics  
Michigan State University, East Lansing, Michigan 48824

and

B.M. Freedom\*\*  
Physics Department, University of South Carolina  
Columbia, South Carolina 29208

NUCLEAR REACTIONS:  $^{37}\text{Cl}(p,d)^{36}\text{Cl}$ ,  $E_p=35$  MeV; measured  $\sigma(E_d, \theta)$ ; deduced excitation energies,  $k_n$ -values and spectroscopic factors for states of  $^{36}\text{Cl}$ . Enriched target.

The  $^{37}\text{Cl}(p,d)^{36}\text{Cl}$  reaction, at  $E_p=35$  MeV, was employed to study properties of the levels of  $^{36}\text{Cl}$ . Excitation energies of levels up to 8.2 MeV were obtained by high-resolution magnetic analysis of the emitted deuterons. Angular distributions for the states observed in this span were measured over the angular range  $\theta_L=3^\circ-55^\circ$ . These data were analyzed with the DWBA theory to obtain values of  $k_n$  and  $C^2S_k$ . The results are compared to the previously extant experimental picture for this nucleus and to predictions of current nuclear structure theory.

\* Research supported in part by the U.S. National Science Foundation.  
\*\* Supported in part by the Research Corporation.

Spectra were recorded with the proportional counter at closely spaced laboratory angles from  $3^\circ$  to  $55^\circ$  with a total resolution of 50 keV (FWHM). The spectrograph acceptance aperture was 0.6 msr for the angular region of greatest importance ( $3^\circ$  to  $30^\circ$ ) and 1.4 msr for angles greater than  $30^\circ$ . The  $^{37}\text{Cl}(p,d)^{36}\text{Cl}$  and  $^{23}\text{Na}(p,d)^{22}\text{Na}$  Q-values dictate an overlap of their separate deuteron spectra for excitations greater than approximately 2 Mev in  $^{36}\text{Cl}$ . Consequently, for higher excitations the counter data generally provided usable cross-section measurements only for those  $^{36}\text{Cl}$  levels separated from others in  $^{36}\text{Cl}$ , and from any in  $^{22}\text{Na}$ , by more than the .50 keV energy resolution for deuterons.

Protons elastically scattered from  $^{37}\text{Cl}$  and  $^{23}\text{Na}$  were observed in an experimental configuration identical to that used in the (p,d) measurements, except for an appropriate adjustment of the spectrograph magnetic field. The  $^{37}\text{Cl}(p,p)^{37}\text{Cl}$  and  $^{23}\text{Na}(p,p)^{23}\text{Na}$  data were recorded at laboratory angles from  $25^\circ$  to  $50^\circ$ . Normalization of the (p,d) cross sections was made relative to these elastic scattering intensities with the assumption that the latter had the cross sections predicted by optical-model calculations made with the Bechetti-Greenlees proton potential<sup>5</sup> (see Table I). A total uncertainty of 15% is estimated from uncorrelated 10% uncertainties in the optical-model predictions and in the normalization procedure itself.

Deuteron spectra were also recorded at angles from  $4^\circ$  to  $45^\circ$  on nuclear emulsion plates. Various runs yielded resolutions of from 10 to 18 keV (FWHM). An example of the best resolution spectra is shown in Figure 1. The spectrograph acceptance

apertures for the plate exposures were the same as those used in recording the counter data. Levels in  $^{36}\text{Cl}$  to approximately 8.2 Mev excitation were observed. At each angle, the deuteron spectrum to roughly 4.8 Mev excitation in  $^{36}\text{Cl}$  was recorded on one 25-cm-long emulsion plate, with the remainder of the deuteron groups and the proton groups from scattering on  $^{12}\text{C}$ ,  $^{16}\text{O}$ ,  $^{23}\text{Na}$ , and  $^{37}\text{Cl}$  falling on a second, adjacent plate.

The relative normalization of all proton and deuteron spectra was determined both by using a NaI monitor detector which measured protons elastically scattered at  $90^\circ$  to the beam direction, and by using a beam-current integrator. Normalization of the plate data to the counter data was accomplished by cross-section comparisons for selected low-lying levels in  $^{36}\text{Cl}$  and  $^{23}\text{Na}$  at several forward angles. The  $^{23}\text{Na}(p,d)^{22}\text{Na}$  angular distributions observed in this experiment show complete consistency in both shape and absolute magnitude with those obtained in another, independent study at this laboratory.<sup>1</sup> When peaks from the  $^{37}\text{Cl}$  and  $^{23}\text{Na}$  reactions coincided, the cross-section associated with the transition to a  $^{36}\text{Cl}$  level was deduced by subtraction of the independently measured  $^{23}\text{Na}(p,d)^{22}\text{Na}$  cross-section for the appropriate energy level and angle. Similar corrections were made for peaks arising from the (p,d) reaction on the residual  $^{35}\text{Cl}$  in the target.

### III. RESULTS

#### III.A Excitation Energies

Excitation energy analysis and assignments were made on the basis of centroids extracted from the best resolution nuclear

emulsion spectra, recorded at 4°, 8°, and 14°. The analysis involved a fit to the particle momenta of the reference states<sup>6,7</sup> listed in Table II via a least-squares adjustment of the beam energy, scattering angle, and the constant, linear, and quadratic coefficients of a  $B_p$  vs. focal-plane-position relationship. The best results were obtained when the mass table Q-values<sup>6</sup> for the  $^{23}\text{Na}(p,d)^{22}\text{Na}$  and  $^{37}\text{Cl}(p,d)^{36}\text{Cl}$  reactions were adjusted by -2 keV and -1 keV, respectively. This is consistent with the adjustment of the  $^{23}\text{Na}(p,d)^{22}\text{Na}$  Q-value required in the analysis of  $^{35}\text{Cl}(p,d)^{34}\text{Cl}$  data,<sup>3</sup> and within the Q-value uncertainties quoted for both reactions. The corrections to the nominal beam energy required by the fits were less than 10 keV, and scattering angle corrections were less than 0.2°. These changes are within the accuracy to which the experimental apparatus and monitoring systems yield precise experimental parameters for any given run.

The excitation energies which were obtained with this procedure are presented in Tables III and IV. Table II indicates some excitation energies in  $^{22}\text{Na}$  simultaneously obtained in the present study in comparison with those found from another investigation with the (p,d) reaction.<sup>1,3</sup> The overall consistency in the energy calibration schemes is evident.

### III.B. Angular Distributions

#### III.B.1 DWBA Analysis

The orbital angular momentum quantum numbers,  $l_n$ , of the neutrons transferred in the (p,d) transitions observed in the present work, and the corresponding spectroscopic factors,  $C^2S_l$ , have been assigned on the basis of fits to the data with distorted-wave-Born approximation (DWBA) angular distributions calculated

using the computer code DWUCK.<sup>8</sup> The optical-model potentials used were of the standard form:

$$U(r) = V_R f(r, a_R) + i(W_V f(r, a_V) - 4W_{SF} a_{SF} \frac{d}{dr} f(r, a_{SF}))$$

$$+ (\frac{\hbar}{m c})^2 V_{SO} \frac{1}{r} \frac{d}{dr} f(r, a_{SO}), \vec{l} \cdot \vec{\sigma}$$

$$\text{where } f(r, a_i) = -[1 + \exp(\frac{r - r_i A^{1/3}}{a_i})]^{-1},$$

$V_R$  is the real well depth,  $W_V$  and  $W_{SF}$  are the volume and surface imaginary well depths, respectively, and  $V_{SO}$  is the strength of the spin-orbit potential. A standard, uniformly charged sphere of radius  $R_c = r_c A^{1/3}$  was used for the Coulomb potential.

The proton optical model parameters of Becchetti and Greenlees<sup>5</sup> were used in all the DWBA calculations presented here. An alternative parameter set presented by Fricke, et al.<sup>9</sup> gave little or no variation of the predicted (p,d) angular distribution shapes. A choice for the deuteron optical-model potential was not so easily made. Deuteron potentials proposed by Perey and Perey,<sup>10</sup> Newman, et al.<sup>11</sup> Hinterberger, et al.<sup>12</sup> Schwandt and Haerberle,<sup>13</sup> and Mermaz, et al.<sup>14</sup> were tested in an effort to reproduce the pure  $l=0$  and  $l=2$  angular distributions experimentally recorded for the (p,d) reaction on several nuclei in the  $32 < A < 39$  region at  $E_p = 35$  MeV.<sup>1-4,15</sup>

This investigation indicated that calculations made in the local, zero-range (LZR) approximation with any of the standard deuteron potentials produce shapes which are inferior to those produced when approximations to finite-range and non-local corrections (FRNL) are introduced. The standard non-locality parameters<sup>8</sup> 0.85 fm and 0.54 fm were chosen for the proton and deuteron,

respectively, while the finite-range parameter<sup>8</sup> for the neutron bound-state was chosen to be 0.621 in all cases. Calculations which employed the "Set 1" parameters of Hinterberger, *et al.*<sup>12</sup> together with the FRNL corrections provided the best overall fits throughout the mass region of any of the above potentials. Even so, the pure  $l=0$  shapes did not completely match the observed  $Q$ -dependence of such distributions, and all calculations tended to predict cross-sections significantly larger than those observed for  $\theta > 35^\circ$ .

Two other approaches to alleviating the deficiencies in the FRNL calculations were investigated. One of these approaches was to employ the "adiabatic" model for (p,d) reactions proposed by Johnson and Soper.<sup>16,17</sup> This model attempts to account for the breakup of the deuteron into a correlated neutron-proton pair and involves abandoning deuteron potentials which reproduce observed elastic scattering in favor of a potential compounded from neutron and proton potentials. Use of the model has produced good results for both light and heavy nuclei.<sup>18,19</sup> The adiabatic-type potentials seem to have the general desirable feature of pulling down the cross-sections at larger angles. However, as we will show, this prescription does not produce significantly better results in the present study than does the conventional prescription when the potentials best founded in terms of the elastic scattering data are used.

The other approach is to take account of a postulated<sup>20</sup> damping of the p-n interaction in the nuclear interior. This procedure has also been shown to improve the general agreement between calculation and experiment for reactions on light nuclei.<sup>21</sup>

The damping factor we employ is of the Fermi form,

$$F(r) = (1.0 - 1.845 \rho(r)^{2/3}),$$

where  $\rho(r) = 0.17 [1 + \exp(x)]^{-1}$ ,  $x = (r - r_0 A^{1/3})/a$ , and " $r_0$ " and " $a$ " are the radius and diffusivity of the neutron bound-state well. The normalization factor suggested by nuclear matter considerations<sup>20</sup> produces an overall renormalization of the calculated DWBA cross-sections, and has been omitted.

The present data have been analyzed in detail using: (1) the Hinterberger "Set 1" deuteron parameters, referred to in the following as FRNL, (2) the same potential parameter set and calculation approximations as in (1) but with the addition of the aforementioned damping correction to the  $V_{pn}$  interaction, referred to in the following as DFRNL, and (3) the adiabatic deuteron prescription in the LZR approximation, henceforth referred to as ADIABATIC. The parameter values are given in Table I.

Angular distributions resulting from these three calculations are compared with each other and with the distributions observed in the present experiment for transitions to four levels in <sup>36</sup>Cl in Figure 2. The DFRNL calculations are seen to yield good fits to the data over a wide range of  $Q$ -values. The ADIABATIC calculations clearly fail to reproduce the shape of the observed  $l=2$  distributions in the  $30^\circ$ - $20^\circ$  region.

### III.B.2 Analysis of Experimental Angular Distributions

The angular distributions observed in this study are shown in Figs. 3, 4 and 5. The curves shown are the result of the DFRNL DWBA calculations. States observed at too few angles for a meaningful attempt to be made at assigning an  $l$ -value are not shown. The

$l_n$ -values and spectroscopic factors for all the states of  $^{36}\text{Cl}$  for which usable angular distributions were measured in the present study are presented in Table V. Attempts to fit a mixture of two  $l_j$  curves were made for each distribution unless known final state spins precluded a possible mixed- $l$  transition; for example, the known ( $J^\pi, \Gamma$ ) = (0, 2), 4299 keV level was fitted only with a pure  $l=2, j=3/2$  calculation. In other cases in Table V where only one  $l$ -value is assigned to a transition, the addition of a second term failed to improve the overall fit.

Absolute spectroscopic factors were extracted from the data by minimizing the quantity

$$\chi^2 = \sum_{i=1}^N \left[ (2.29c^2 S_{ij})^2 \frac{d\sigma(\theta_i)}{d\Omega} - \frac{d\sigma(\theta_i)}{d\Omega} \right]^2$$

where, as noted,  $l=0$  and 2 or 1 and 3, over the  $N$  data points in the  $\theta_{i=1}$  to  $\theta_{i=N}$  region. The bulk of the spectroscopic factors were converted to a relative scale described in the following section. A comparison of the spectroscopic factors obtained from the present data with the DFRNL, FRNL, and ADIABATIC calculations, together with those obtained from other single neutron pick-up experiments on  $^{37}\text{Cl}$ , is presented in Table VI.

#### IV. DISCUSSION

IV.A. Energy Levels and Assignments of  $l_n$  and  $J^\pi$  for Levels Below 5.6 MeV Excitation

The levels of  $^{36}\text{Cl}$  observed below 5.6 MeV excitation are compared to the composite set of levels compiled by Endt and van der Leun<sup>7</sup> in Table III. Of the 51 levels which they list in this region,

we observe definite evidence for 32. We also note clear evidence for 5 levels in this region which they do not list in their compilation. Of these 5 levels, 3 have antecedents in the literature<sup>22-30</sup> from which the compilation of Ref. 7 was drawn. The levels we observe at  $E_x=3566$ , 4524, and 5249 keV have plausible counterparts in the ( $n, \gamma$ ) results of Alves, *et al.*<sup>22</sup> One of our two levels at 4720 and 4738 keV seems to correspond to the one observed in the ( $d, p$ ) reaction,<sup>23,7</sup> at 4726 keV and the other is previously unobserved. The other previously unobserved level occurs at 4205 keV, and is assigned (1,2)<sup>+</sup> on the basis of its  $l_n=0+2$  angular distributions.

It is not clear whether there exist one or two levels in the 3470 keV region. We observe only one, with  $l=0+2$ , at 3470 keV. This level must correspond to the 3497 keV level listed in Ref. 7 (taken from Ref. 28) and to the 3477 keV level noted in Ref. 24. The 3468 keV level<sup>7</sup> (noted in the ( $d, p$ ) work of Ref. 23) is assigned  $l=1$  with a very weak strength. This state could perhaps be the positive-parity state we observe, or there could be two different states at this energy.

Two of the  $J^\pi$  assignments listed in Ref. 7 for this region are ostensibly contradicted by the present results. One involves the level at 3470 keV just mentioned. The second conflict involves the state at 2863 keV. Our results show a reasonable strong distribution completely typical of  $l_n=2$  transfer. The grounds for the  $J^\pi=3^-$  assignment to a level at 2864 keV would seem to be solid also. This conflict can most easily be resolved by postulating a doublet at this excitation energy.

The agreement between the consensus energies arrived at in Ref. 7 and those assigned in this work, with no reference to any previous data on the  $^{36}\text{Cl}$  level spectrum, is excellent up through 5.6 MeV excitation. Above 2.5 MeV excitation the uncertainties of the present values are generally smaller than those of the older values. The present results have the additional virtues of comprising a large fraction of the total number of levels and of treating this sample in a completely self-consistent fashion. The relative difference in the present excitation values between levels  $\leq 1$  MeV apart should always be less than 2 keV.

One rather significant change in excitation energy from Ref. 7 is that the excitation of the lowest  $T=2$  state is moved down from 4323 to 4299 keV. This change is consistent with the results of Ref. 24. The state listed in Ref. 7 at 2892 keV almost certainly corresponds to the one we observed at 2863 keV. We failed to resolve the 1952-1960 keV doublet in the present study, but the lack of broadening in the 1958 keV peak we observe indicates that the negative-parity contributions to the observed differential cross sections are insignificant. Finally, we were unsuccessful in finding a match for the  $0^+$  level observed at 3.12 MeV in the ( $^3\text{p}, \text{He}$ ) reaction on  $^{38}\text{Ar}$ .<sup>25</sup>

The positive-parity assignments we make in Table III seem quite secure. The evidence for these assignments, shown in Figs. 3 and 4, should be convincing. The negative-parity assignments, based on the results shown in Fig. 5, are much less solid. The calculated and (presumed) experimental  $l_n=3$  angular distributions

are each rather structureless, yet not quite in good agreement with each other. Shell-model arguments, not comparison to DWBA curves, rule out  $l_n=4$  assignments to some " $l_n=3$ " distributions. Some  $l_n=1$  distributions can be assigned unambiguously, but others are so weak or so mixed with  $l_n=3$  that the present assignments are not conclusive. However, all of our negative parity assignments agree with the assignments from ( $d,p$ ) reaction studies.

#### IV.B Energy Levels and Assignments of $l_n$ and $J^\pi$ for Levels Between 5.6 and 8.2 MeV Excitation

We observe 30 states between 5.6 and 8.2 MeV excitation energy, ten of which have not been previously been reported. The results are compared to previous work in Table IV. The uncertainties in the energy values obtained in the present work are considerably smaller than those of the prior studies. Assignments of  $l_n$  (and consequent limits on  $J$ ) are made to almost all levels observed in this region. Eighteen reasonably secure positive-parity assignments are obtained, and several believable negative-parity assignments. There are three disagreements with previous work. The level at 5734 keV has a very well defined  $l_n=3$  shape, in conflict with the  $l_n=2$  assignment of Ref. 27. The levels at 5913 and 6095 keV, assigned in Ref. 23 as  $l_n=1$ , are seen here to be  $l_n=0^+$ 2.

#### IV.C. Values of $C^2S$

The spectroscopic factors listed in Tables V, VI, and VII are normalized such that the ground-state values equal 1.10. The absolute values obtained in our analysis are quite a bit larger, as can be seen from the unnormalized ground state values listed in Table VI. The approach we employ here is to set one of

the best determined experimental values equal to a theoretical value which is essentially invariant among a wide variety of structure calculations. Hence our attention is directed solely to the relative values of the spectroscopic factors normalized to this reference level.

The spectroscopic factors listed in Table V sum up to values of 7.14 for  $\lambda=2$ , 1.23 for  $\lambda=0$ , 0.69 for  $\lambda=3$ , and 0.15 for  $\lambda=1$ . It is impossible to distinguish between  $d_{5/2}$  and  $d_{3/2}$  transfer from the experimental data. All analysis has assumed  $d_{3/2}$  pickup. If a particular level is actually populated by  $d_{5/2}$  pickup, the spectroscopic factor would be 0.85 as large as that listed.

The sum of  $\lambda=2$  strength should be considered an upper limit, since for strong  $\lambda=0$  transitions, a significant amount of  $\lambda=2$  strength can be assigned by our objective fitting procedure because such an addition serves to compensate for imperfections in the fit of the theoretical  $\lambda=0$  shape to the experimental  $\lambda=0$  distributions.

The amount of  $\lambda=0$  strength assigned in the present analysis is unambiguous because of the dominance of the  $\lambda=0$  shape at small angles and because the present data completely cover the small-angle region. The sum of  $\lambda=3$  strength should be considered an upper limit only, since the  $\lambda=3$  shape is quite structureless and a significant fraction of the extracted  $\lambda=3$  strength thus probably corresponds to reaction cross sections which do not necessarily arise from direct  $f_{7/2}$  pickup. We would estimate that about half of the total  $\lambda=3$  strength can be safely attributed to real  $f_{7/2}$  admixtures in the  $^{37}\text{Cl}$  ground state. The  $\lambda=1$  strength observed, 0.15 in magnitude is not well fixed. Again, maybe half of the tabulated strength is unambiguously there.

The consistency with which spectroscopic factors can be extracted from the present data by different analytical procedures, and the consistency between the present results and past determinations can be inspected in Table VI. With respect to the present data we see that the largest inconsistencies arise for the  $\lambda=2$  contributions assigned to distributions dominated by  $\lambda=0$ . These effects are caused by the varying success of the three DWBA calculations in fitting the pure  $\lambda=0$  shapes. Inspection of the values for pure  $\lambda=2$  transitions indicates 15% inconsistencies in the Q-dependence of the calculated cross sections.

The agreement of the present results with previous work is good for strong transitions dominated by  $\lambda=2$ . Significant deviations occur for  $\lambda=0$  strengths. We attribute these in the main to the inadequate sampling of the  $\lambda=0$  maximum in previous work. In several instances, previous work did not even detect  $\lambda=0$  components which are obvious in the present data.

#### IV.D. Theoretical Discussion

The results of the present investigation are compared to results of theoretical calculations made in a full  $d_{5/2}^{-1} s_{1/2}^{-1} d_{3/2}$  shell-model space<sup>32</sup> in Table VII. All theories for  $^{36}\text{Cl}$  predict the structure of the first two levels to be dominated by the  $(d_{3/2})^{-4} J=2$  and  $3 T=1$  configurations; the ratio of spectroscopic factors 1.1/1.6 then follows. All experimental results confirm this picture. The theoretical numbers listed in Table VII are the average of the results from the two most



successful Hamiltonians investigated in Ref. 32. After the first two levels, even these two closely related calculations, quite similar in most of their predictions, do not yield stably consistent results from the levels of  $^{36}\text{Cl}$ . We have juxtaposed the average theoretical energies and spectroscopic factors in a way that seems most plausible to us. This involves reassigning the 1600 keV state to  $1^+$  following the suggestion of Vernotte.<sup>33</sup> The theoretical results (energies and spectroscopic factors) are in reasonable agreement with the present results for the first six positive-parity levels. The correspondances of Table VII strongly suggest that the 2863 keV level is  $3^+$ .

The calculations predict that essentially all the  $d_{3/2}$  hole strength for  $J^\pi = 2$  and  $3$ ,  $T=1$  goes into the ground and first excited states. Higher lying  $\ell=2$  strength to  $2^+$  and  $3^+$   $T=1$  states is almost all  $d_{5/2}$ . The  $d_{3/2}$  strength to  $1^+$  levels is predicted to be highly fragmented, however. The present experimental results agree with, or where the issue cannot be decided definitively, are consistent with, these predictions. The calculations correctly predict that the  $1^+$  state dominated by  $d_{3/2}$  pickup is the lowest one.

The calculations predict that essentially all of the  $d_{3/2}$  neutron pickup strength ( $C^2S=4$ ) should be observed in the low-lying levels observed in the present study. Based on our ground-state-normalized values, we clearly observe more  $\ell=2$  strength than the sum-rule limit for  $d_{3/2}$ , even allowing for some over-estimation of this quantity. The calculations predict that an amount

of  $d_{5/2}$  strength roughly equivalent to the excess over  $4$  which we observe should occur in this same region. Thus the  $\ell=2$  spectroscopic factors extracted from the present data agree with the gross summed-strength predictions of the sd-shell model predictions and with the detailed distributions predicted for the low-lying levels. Structure calculations which ignore  $d_{5/2}$  excitations cannot possibly reproduce all these effects.

The total  $\ell=0$  strength extracted from the present data is  $\sim 1.2$ . The amount of spectroscopic strength for  $\ell=0$  neutron pickup predicted for the present region of observation by the shell-model calculations is  $\sim 1.3$  out of the limit of 2. Again, as can be noted in Table VII, the observed detailed distribution of this strength is also correctly predicted by the calculations.

Above 4 MeV excitation the present results indicate significantly more positive-parity states than an sd-shell basis can account for. To generate the requisite density of levels, structure theories must allow for excitations into the fp-shell. Calculations, such as those of Erne,<sup>34</sup> indicate that the observed level densities, at least, are easily obtained. The "extra" or "intruder" positive-parity states serve to fragment the sd-shell pickup strength predicted by a purely sd-shell calculation to occur in a single state. A probable example of this effect occurs in the case of the large  $d_{5/2}$ -pickup strength predicted<sup>32</sup> for the third sd-shell-model  $4^+$ ,  $T=1$  state. No single state with a majority of the predicted strength is observed, but several pure  $\ell=2$  states whose combined spectroscopic factors are of the correct magnitude are found in the right energy region. As a

final comment on this general question we might note that the amount of fp-shell admixture assigned to the ground state of  $^{37}\text{Cl}$  in the present study by virtue of the sum of the observed  $\lambda_n=1$  and 3 strength is consistent with that obtained for  $^{39}\text{K}$  in a similar investigation.<sup>2</sup>

#### V. CONCLUSIONS

The excitation energies of states of  $^{36}\text{Cl}$  measured in this experiment, together with the associated  $l$ -values and spectroscopic factors for neutron pickup, serve to make more precise and clear the energy level scheme for this nucleus. The measured angular distributions are fitted quite well with orthodox applications of DWBA theory, and the uncertainties in extracted spectroscopic factors are typical of any kind of direct reaction.

Aside from the first  $1^+$  and  $2^+$ ,  $T=1$  states, the first two  $3^+$ ,  $T=1$  states, and the first  $0^+$  and  $2^+$ ,  $T=2$  states, the structure of the positive-parity levels of  $^{36}\text{Cl}$  seems quite complex. Other than for these states, similar theoretical calculations yield rather divergent results, and experiment fails to definitively select any single theoretical construct as best. The experimental results agree with an "average" theory for the lowest six or seven levels of  $^{36}\text{Cl}$ , but from that point on, detailed comparison is in general not possible.

Thus, while the (p,d) results validate the basic elements of the current shell-model predictions for  $^{36}\text{Cl}$ , they indicate

that a more accurate accounting of the 2-4 MeV region of excitation is needed. Above this excitation energy, detailed explanation of the theoretical spectrum will necessarily involve explicit consideration of fp-shell excitations.

## REFERENCES

1. B.H. Wildenthal, J.A. Rice, and B.M. Freedom, to be published.
2. B.H. Wildenthal, J.A. Rice, and B.M. Freedom, to be published, and Bull. Am. Phys. Soc. 17, 554(1972).
3. B.H. Wildenthal, J.A. Rice, and B.M. Freedom, to be published, and Bull. Am. Phys. Soc. 17, 485(1972).
4. D.A. Show, B.H. Wildenthal, J.A. Nolen, and E. Kashy, to be published, and Bull. Am. Phys. Soc. 17, 533(1972).
5. F.D. Becchetti and G.W. Greenlees, Phys. Rev. 182, 1190(1969).
6. A.H. Wapstra and N.B. Gove, Nuclear Data Tables, Vol. 9, Numbers 4-5, July 1971.
7. P.M. Endt and C. van der Leun, Nuclear Physics A214, 1(1973).
8. P.D. Kunz, unpublished.
9. M.P. Fricke, E.E. Gross, B.J. Morton, and A. Zucker, Phys. Rev. 156, 1207(1967).
10. C.M. Perey and F.G. Perey, Phys. Rev. 152, 923(1966).
11. E. Newman, L.C. Becker, B.M. Freedom, and J.C. Hiebert, Nucl. Phys. A100, 225(1967).
12. F. Hinterberger, G. Mairle, V. Schmidt-Rohr, G.J. Wagner, and P. Turek, Nucl. Phys. A111, 265(1968).
13. P. Schwandt and W. Haerberli, Nucl. Phys. A123, 401(1969).
14. M.C. Mermaz, C.A. Whitten, J.W. Champain, A.J. Howard, and D.A. Bromley, Phys. Rev. C4, 1778(1971).
15. A. Moalem and B.H. Wildenthal, to be published.
16. R.C. Johnson and P.J.R. Soper, Phys. Rev. C1, 976(1970).
17. J.D. Harvey and R.C. Johnson, Phys. Rev. C3, 636(1971).
18. G.M. McAllen, W.T. Pinkston, and G.R. Satchler, Particles and Nuclei 1, 412(1971).
19. G.R. Satchler, Phys. Rev. C4, 1485(1971).
20. A.M. Green, Phys. Letters 24B, 384(1967).
21. B.M. Freedom, Phys. Rev. C5, 587(1972); and B.M. Freedom, J.L. Snelgrove and E. Kashy, Phys. Rev. C1, 1132(1970).
22. R.N. Alves, J.M. Kuckly, J. Julien, C. Samour, and J. Morgenstern, Nucl. Phys. A135, 241(1969).
23. A.M. Hoogenboom, E. Kashy, and W.W. Buechner, Phys. Rev. 128, 305(1962).
24. J. Kroon, B. Hird, and G.C. Ball, Nucl. Phys. A204, 609(1973).
25. J.C. Hardy, H. Brunnader, and J. Cerny, Phys. Rev. C1, 561(1970).
26. P. Decowski, Nucl. Phys. A169, 513(1971).
27. G. Ronsin, M. Vergnes, G. Rotbard, J. Kalifa, and I. Linck, Nucl. Phys. A187, 96(1972).
28. B. Vignon, J.P. Longqueue, and I.S. Towner, Nucl. Phys. A189, 513(1972).
29. Lars Broman, C.M. Fou, and Baruch Rosner, Nucl. Phys. A112, 195(1968).
30. J. Honzatko, J. Kajfosz, and Z. Kosina, Nucl. Phys. A174, 668(1971).
31. G. van Middelkoop and P. Spilling, Nucl. Phys. 77, 267(1966).
32. B.H. Wildenthal, E.C. Halbert, J.B. McGroory, and T.T.S. Kuo, Phys. Rev. C4, 1266(1971).
33. J. Vernotte, private communication.
34. F.C. Erne, Nucl. Phys. 84, 91(1966).

Table I. Optical-model parameters used in the analysis of the  $^{37}\text{Cl}(p,d)^{36}\text{Cl}$  data.

Particle	$V_R$ (MeV)	$r_R$ (fm)	$a_R$ (fm)	$W_V$ (MeV)	$r_V$ (fm)	$a_V$ (fm)	$W_{SF}$ (MeV)	$r_{SF}$ (fm)	$a_{SF}$ (fm)	$V_{SO}$ (MeV)	$r_{SO}$ (fm)	$a_{SO}$ (fm)	$r_C$ (fm)
Proton <sup>a</sup>	46.79	1.17	0.75	5.0	1.32	0.57	4.02	1.32	0.57	6.2	1.01	0.75	1.17
Deuteron <sup>b</sup> (FRNL and DFRNL)	86.73-0.35E <sub>cm</sub>	1.25	0.73				13.0	1.25	0.761	6.0	1.25	0.73	1.30
Deuteron <sup>c</sup> (ADIABATIC)	102.76 <sup>d</sup>	1.17	0.779	1.60 <sup>d</sup>	1.29	0.603	16.91 <sup>d</sup>	1.29	0.597	6.2	1.01	0.75	1.17
Neutron Bound State	Adjusted to match separa- tion energy	1.24	0.65							$\lambda=25$			1.24

<sup>a</sup>Ref. 5.<sup>b</sup>Ref. 12.<sup>c</sup>Ref. 16,18 proton and neutron parameters from Reference 5.<sup>d</sup>Values shown are for  $E_x=0.000$  MeV only; Q-dependence is as given in Reference 5.Table II. States used for the energy calibration of the  $^{37}\text{Cl}(p,d)^{36}\text{Cl}$  reaction data. Some energies in  $^{22}\text{Na}$  extracted in the present work and in a previous (p,d) study are shown to illustrate calibration consistency.

Reaction	Excitation Energy (keV) in the Residual Nucleus <sup>a</sup>	Levels in $^{22}\text{Na}$ (keV) from previous work <sup>b</sup>	Levels in $^{22}\text{Na}$ (keV) from this work
$^{37}\text{Cl}(p,d)^{36}\text{Cl}$	(Q=-8,088 keV) <sup>c</sup>		
$^{23}\text{Na}(p,d)^{22}\text{Na}$	(Q=-10,195 keV)	000, +1	000
	583.05 ± 0.14 <sup>d</sup>	583 ± 1	583 ± 1
	657.0 ± 0.14 <sup>d</sup>	657 ± 1	658 ± 1
	890.89 ± 0.2 <sup>d</sup>	891 ± 1	890 ± 1
	1951.8 ± 0.3 <sup>d</sup>	1952 ± 1	1952 ± 2
	1983.5 ± 0.5 <sup>d</sup>	1984 ± 1	1984 ± 2
	2211.4 ± 0.32 <sup>d</sup>	2211 ± 1	2211 ± 2
	2571.5 ± 0.3 <sup>d</sup>	2571 ± 1	2571 ± 2
	2968.6 ± 0.6 <sup>d</sup>	2968 ± 2	2971 ± 4
	3059.4 ± 0.6 <sup>d</sup>	3059 ± 1	3061 ± 4
		3943 ± 2	3944 ± 4
		4072 ± 2	4072 ± 4
		4583 ± 2	4581 ± 4
		5958 ± 4	5959 ± 5
		5992 ± 4	5993 ± 5
$^{16}\text{O}(p,d)^{15}\text{O}$	(Q=-13,444.8 keV) <sup>e</sup>		
$^{12}\text{C}(p,d)^{11}\text{C}$	(Q=-16,497.2 keV) <sup>e</sup>		
$^{37}\text{Cl}(p,d)^{36}\text{Cl}$	ground state		
$^{23}\text{Na}(p,p)^{23}\text{Na}$	ground state		
	439.9 ± 0.2 <sup>d</sup>		
$^{16}\text{O}(p,p)^{16}\text{O}$	ground state		
$^{12}\text{C}(p,p)^{12}\text{C}$	ground state		

<sup>a</sup>Used for present calibration.<sup>b</sup>Reference 1.<sup>c</sup>Adjusted as described in text from the values of Ref. 6.<sup>d</sup>Reference 7.<sup>e</sup>Reference 6.

Table III. Levels of  $^{36}\text{Cl}$  below 5.6 MeV excitation energy as observed in the present study and as compiled from previous measurements.

$E_x^a$	$J^\pi$	$E_x^b$	$J^\pi$	$E_x^a$	$J^\pi$	$E_x^b$	$J^\pi$
0	2 <sup>+</sup>	0	2 <sup>+</sup>	4030±5	1	4035 ±5	(0-3) <sup>-</sup>
789±1	2	789.2±0.2	3 <sup>+</sup>			4139.2±0.4	(1-3) <sup>-</sup>
1165±1	0 <sup>+</sup>	1164.9±0.2	1 <sup>+</sup>	4205±4	0 <sup>+</sup>		
1600±1	0 <sup>+</sup>	1601.1±0.2	2 <sup>+</sup>	4299±3	2	4323 ±14	0 <sup>+</sup> (T=2)
		1951.6±0.2	2 <sup>-</sup>	4316±4		4316 ±7	(0-3) <sup>-</sup>
1958±1	0 <sup>+</sup>	1959.6±0.2	2 <sup>+</sup>			4406 ±8	
2467±2	1	2468.6±0.2	3 <sup>-</sup>			4497 ±2	(1-3) <sup>-</sup>
2491±2	0 <sup>+</sup>	2491 ±2	(1,2) <sup>+</sup>	4524±4	1+3	4526 ±8 <sup>c</sup>	
2517±2	3	2517 ±5	(1-5) <sup>-</sup>	4551±4	0+2	4553 ±8	(1,2) <sup>+</sup>
2675±2	0 <sup>+</sup>	2677 ±2	(0-4) <sup>+</sup>			4599 ±2	(1,3) <sup>-</sup>
2799±3	3	2812 ±5	(2-4) <sup>-</sup>	4720±4			
2863±2	2	2864 ±2	3 <sup>-</sup>	4738±5		4726 ±8	(1-5) <sup>-</sup>
		2892 ±17	(0-4) <sup>+</sup>			4757 ±2	(1-3) <sup>-</sup>
2894±2		2896 ±5	(1-3) <sup>-</sup>	4830±5	1+3	4826 ±8	
2995±2	(1+3)	2995 ±2	(1-3) <sup>-</sup>	4852±4	1+3	4849 ±8	
		3100 ±5	(2-4) <sup>-</sup>	4884±4	0+2	4879 ±8	
		3120 ±100	0 <sup>+</sup>	4953±5		4957 ±8	(0-3) <sup>-</sup>
3208±4	1	3207 ±6	(0-2) <sup>-</sup>			5000 ±8	(0-3) <sup>-</sup>
3331±3	1	3334 ±2	(1-3) <sup>-</sup>			5082 ±8	(0-3) <sup>-</sup>
3470±3	0 <sup>+</sup>	3468 ±5	(1-3) <sup>-</sup>	5144±6	1+3	5152 ±2	
		3497 ±16	(1,2) <sup>+</sup>				
3566±4	0+2	3564 ±8 <sup>c</sup>				5205 ±2	(1-3) <sup>-</sup>
3598±3	(1+3)	3601 ±2	(2,3) <sup>-</sup>	5249±5	(1+3)	5250 ±8 <sup>c</sup>	
		3633.6±0.2	(1,2) <sup>-</sup>			5261 ±8	(0-3) <sup>-</sup>
(3661)		3666 ±6				5306 ±8	(0-3) <sup>-</sup>
3722±4	3	3724 ±5	(1-5) <sup>-</sup>			5331 ±8	
		3825 ±5				5461 ±2	(1-3) <sup>-</sup>
3962±4	1+3	3964.5±0.5	(1-3) <sup>-</sup>	5517±5	1+3	5517 ±2	(2,3) <sup>-</sup>
3990±4	1	3994 ±2	(1-3) <sup>-</sup>				

<sup>a</sup>Present work.

<sup>b</sup>Ref. 7.

<sup>c</sup>Ref. 22.

<sup>d</sup>Ref. 23.

Table IV. Levels of  $^{36}\text{Cl}$  between 5.6 and 8.2 MeV excitation energies.

$E_x^a$	$J^\pi$	$E_x^b$	$J^\pi$	$E_x^c$	$J^\pi$
5605±5	0+2	(5622)			
5702±5	1+3	5701	1		
5734±6	3	5731		573(0)	
5873±5	0+2	5906	1		
5957±5	0+2	5952			
5986±5	(1+3)	(5972)		600(0)	
6095±5	0+2	6090	1		
6146±5	0+2	(6155)		615(0)	
6184±5	0+2			619(0)	
6354±6	0+2	6356			
6379±5	0+2				
6423±5	1+3			645(0)	
6480±7	1+3	6474		649(0)	
6550±5	0+2	6546		654(0)	
6596±7	1+3				
6618±5	2				
6683±5	1+3			668(0)	
6750±6	0+2			675(0)	
6774±6	2				
6826±6	2			684(0)	
6893±7	0+2			689(0)	
7007±6					
7088±6	2			709(0)	
7165±7				716(0)	
7512±6	0+2				
7557±6	0+2				
7665±6	0+2			764(0)	
7755±6	1+3				
7870±6	0+2				
8184±6	(0+2)				

<sup>a</sup>Present work.

<sup>c</sup>Ref. 29.

<sup>b</sup>Ref. 23 (±8 keV).

Table VI. Experimental values of  $C^2S_{\lambda}$  for transitions from  $^{37}\text{Cl}$  to  $^{36}\text{Cl}$ . Absolute values for the ground state are presented in parentheses. All other values are normalized such that  $C^2S_{\lambda} = 1.10$  for the ground state.

$E_x(\text{keV})^a$	$J^{\pi}, T$	$\lambda^a$	DFRNL <sup>a</sup>	FRNL <sup>a</sup>	ADIABATIC <sup>a</sup>	(p,d) <sup>b</sup>	( $^3\text{He}, \alpha$ ) <sup>c</sup>	( $^3\text{He}, \alpha$ ) <sup>d</sup>	(p,d) <sup>e</sup>
000	2 <sup>+</sup> , 1	2	(2.36)	(1.85)	(2.08)		(0.92)	(1.30)	(0.90)
789	3 <sup>+</sup> , 1	2	1.10	1.10	1.10	1.10	1.10	1.10	1.10
1165	1 <sup>+</sup> , 1	0	0.05	0.05	0.06	0.07	<0.13		0.18
1600	(1,2) <sup>+</sup> , 1	2	0.36	0.35	0.35	0.35	0.35	0.37	0.49
1958	2 <sup>+</sup> , 1	0	0.16	0.19	0.14	0.28	0.28-0.11	0.19	0.31
2491	(1,2) <sup>+</sup> , 1	2	0.11	0.06	0.15	<0.11	<0.15		
2675	(1) <sup>+</sup> , 1	0	0.23	0.27	0.20	0.47	0.37-0.20	0.42	0.79
2863	(0-4) <sup>+</sup> , 1	2	0.24	0.16	0.31	<0.19	0.15-0.31		
3470	(1,2) <sup>+</sup> , 1	0	0.17	0.20	0.14	0.34	0.32-0.16	0.38	
3722	(2-5) <sup>-</sup> , 1	2	0.19	0.12	0.23	<0.14	0.21-0.25		
4299	0 <sup>+</sup> , 2	0	0.07	0.07	0.07				
4884	(1,2) <sup>+</sup> , 1	2	0.31	0.27	0.32	0.34	0.41	0.37	
5734	(2-5) <sup>-</sup> , 1	0	0.45	0.38	0.41	0.47	0.37	0.38	
6826	(0-3) <sup>+</sup> , 1	2	0.05	0.06	0.04	0.11	0.08	0.15	
7557	2 <sup>+</sup> , 2	2	0.07	0.05	0.09	<0.04	0.08		
		3	0.04	0.03	0.03		0.10g	0.05	
		2	0.29	0.24	0.27	0.31	0.45	0.30	
		0	0.05	0.06	0.04		0.14		
		2	0.05	0.02	0.07		0.09		
		3	0.09	0.07	0.08		0.25h		
		2	0.36	0.26	0.41		0.43		
		0	0.18	0.18	0.13		0.28		
		2	0.18	<0.01	0.27				

<sup>a</sup>Present work.

<sup>b</sup>Reference 24.

<sup>c</sup>Reference 27.

<sup>d</sup>Reference 29.

<sup>e</sup>Reference 28.

g<sub>l</sub>=1

h<sub>l</sub>=2

Table V. Experimental values of  $\lambda$  and  $C^2S_{\lambda}$  for the  $^{37}\text{Cl}(p,d)^{36}\text{Cl}$  reaction as observed in the present investigation. All assignments are based on the DFRNL analysis, with the spectroscopic factors normalized to yield  $C^2S_{\lambda} = 1.10$  for the transition to the  $^{36}\text{Cl}$  ground state.

$E_x(\text{keV})$	$\lambda$	$C^2S_{\lambda}$	$E_x(\text{keV})$	$\lambda$	$C^2S_{\lambda}$
000	2	1.10	5249	(1,3)	<0.01, 0.01
789	2	1.66	5517	1,3	<0.01, 0.02
1165	0,2	0.05, 0.36	5605	0,2	0.02, 0.04
1600	0,2	0.16, 0.11	5702	1,3	0.02, 0.02
1958	0,2	0.23, 0.24	5734	3	0.09
2467	1	0.01	5913	0,2	0.01, 0.04
2491	0,2	0.17, 0.19	5957	0,2	0.01, 0.05
2517	(3)	0.05	5986	(1,3)	<0.01, 0.02
2675	0,2	0.07, 0.31	6095	0,2	0.02, 0.15
2799	(3)	0.05	6146	0,2	0.01, 0.05
2863	2	0.45	6184	0,2	0.01, 0.07
2995	1,3	<0.01, 0.01	6354	0,2	0.02, 0.04
3208	1	<0.01	6379	0,2	0.03, 0.18
3331	1	0.01	6423	1,3	<0.01, 0.08
3470	0,2	0.05, 0.07	6480	1,3	0.02, 0.15
3566	0,2	0.01, 0.01	6550	0,2	0.01, 0.01
3598	(1,3)	<0.01, 0.02	6596	1,3	<0.01, 0.02
3722	3	0.04	6618	2	0.15
3962	1,3	<0.01, 0.01	6683	1,3	<0.01, 0.07
3990	1	<0.01	6750	0,2	0.01, 0.05
4030	1	<0.01	6774	2	0.31
4205	0,2	0.01, 0.04	6826	2	0.36
4299	0,2	0.01, 0.29	6893	0,2	0.02, 0.04
4524	1,3	0.01, 0.04	7088	2	0.22
4551	0,2	0.04, 0.06	7512	0,2	0.01, 0.06
4830	1,3	0.01, 0.02	7557	0,2	0.18, 0.18
4852	1,3	<0.01, 0.01	7665	0,2	0.01, 0.02
4884	0,2	0.05, 0.05	7755	1,3	<0.01, 0.04
5144	1,3	<0.01, 0.01	7870	0,2	0.02, 0.02
			8184	(0,2)	<0.01, 0.04

<sup>a</sup>Values for  $\lambda=0,1,2,3$  are for  $2s_{1/2}$ ,  $2p_{3/2}$ ,  $1d_{3/2}$  and  $1f_{7/2}$  calculations, respectively.

Table VII. Comparison of pickup spectroscopic factors measured for states of  $^{36}\text{Cl}$  with theoretical values.

$E_x$ (keV) <sup>a</sup>	$J^\pi, T^{a,b}$	$(100[C^2S(0)]^a/C^2S(2)]$	$E_x$	$J^\pi, T^c$
	expt. <sup>a</sup>	calc. <sup>c</sup>		
000	$2^+$	/110	/110	$0.00$ $2^+, 1$
789	$3^+, 1$	/166	/155	$0.91$ $3^+, 1$
1165	$1^+, 1$	5/36	4/35	$1.00$ $1^+, 1$
1600	$1^+, 1^d$	16/11	9/9	$2.01$ $1^+, 1$
1958	$2^+, 1$	23/24	17/20	$1.65$ $2^+, 1$
2491	$(1,2)^+, 1$	17/19	23/9	$2.22$ $2^+, 1$
2675	$(1,2)^+, 1$	7/31	1/9	$2.60$ $1^+, 1$
2863	$(0-4)^+, 1$	/45	/65	$2.44$ $3^+, 1$
2894	$(0-4)^+, 1$	/3	/2	$2.75$ $0^+, 1$
3470	$(1-2)^+, 1$	5/7		
3566	$(1,2)^+, 1$	1/1		
4205	$(1,2)^+$	1/4		
4299	$0^+, 2$	/29	/22	$0^+, 2$
6095	$(1,2)^+$	2/15	/21	$4.84$ $3^+, 1$
6379	$(1,2)^+$	3/18		
6618	$(0-4)^+$	/13		
6774	$(0-4)^+$	/31	/120	$6.2$ $4^+, 1$
6826	$(0-4)^+$	/36		
7088	$(0-4)^+$	/22		
7557	$2^+, 2$	18/18	27/4	$2^+, 2$

<sup>a</sup>Present work.

<sup>b</sup>Ref. 7.

<sup>c</sup>Ref. 32.

<sup>d</sup>Ref. 33.

FIGURE CAPTIONS

Figure 1: A spectrum from the (p,d) reaction on the  $^{23}\text{Na}-^{37}\text{Cl}$  target, measured at 35 MeV and  $14^\circ$ , as recorded on nuclear emulsion plates. The resolution of the deuteron groups is 10 keV, FWHM. All excitation energy values are from the present work, with those "boxed" indicating levels in  $^{36}\text{Cl}$ .

Figure 2: A comparison of fits to representative angular distributions with the three chosen types of DWBA calculations. All fits were performed over the angular range from  $3^\circ$  to  $35^\circ$ . The curves are identified as follows: —DFRNL, ----FRNL and ---ADIABATIC.

Figure 3: Experimental angular distributions of strongly excited states in  $^{36}\text{Cl}$  which are assigned positive parity. The solid curves are fits of the DFRNL calculations to the data in the angular range from  $3^\circ$  to  $35^\circ$ . The dotted curves indicate the contributions of the  $\ell=0$  distributions.

Figure 4: Experimental angular distributions of weakly excited states in  $^{36}\text{Cl}$  which are assigned positive parity. The solid curves are fits of the DFRNL calculations to the data in the angular range from  $3^\circ$  to  $35^\circ$ . The dotted curves indicate the contributions of the  $\ell=0$  distributions.

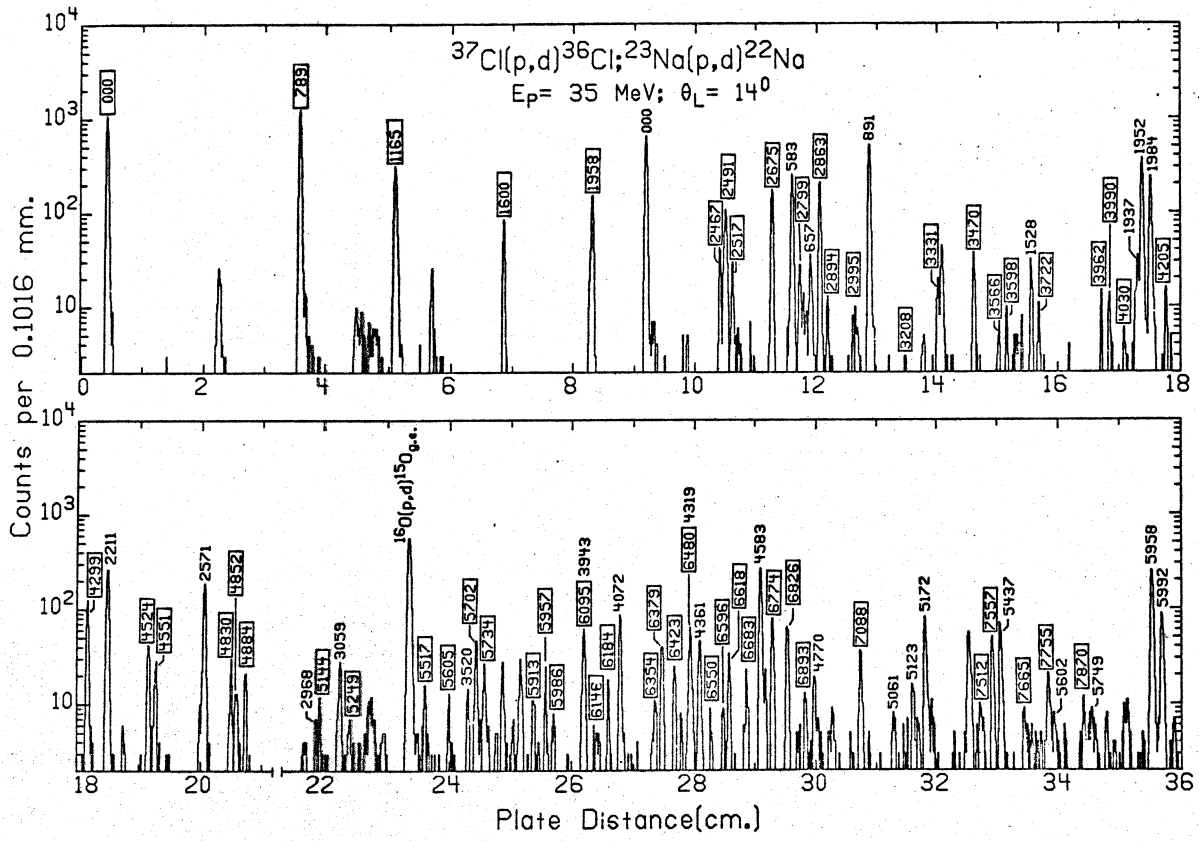


Figure 5: Experimental angular distributions of states in  $^{36}\text{Cl}$  which are assigned negative parity. The solid lines are the fits of the DFRNL calculations to the data in the range from  $3^\circ$  to  $35^\circ$ . The dotted curves indicate the contributions of the  $l=1$  distributions.



